ELSEVIER

Journal of Chromatography A, 855 (1999) 71–89

JOURNAL OF CHROMATOGRAPHY A

www.elsevier.com/locate/chroma

Optimization of throughput and desorbent consumption in simulated moving-bed chromatography for paclitaxel purification

D.-J. Wu[a], Z. Ma[b], N.-H.L. Wang[a,*]

[a]*School of Chemical Engineering, Purdue University, West Lafayette, IN 47907, USA*
[b]*Bioanalytical Systems, Inc., West Lafayette, IN 47906, USA*

Received 6 May 1999; received in revised form 11 May 1999; accepted 11 May 1999

Abstract

In simulated moving-bed (SMB) applications, throughput and desorbent consumption are two key factors that control process cost. For a given adsorbent volume and product purity requirements, throughput and desorbent consumption depend on desorbent composition, column configuration, column length to diameter ratio, and adsorbent particle size. In this study, these design parameters are systematically examined for paclitaxel purification. The results show that if adsorbent particle size, column dimensions and column configuration are fixed, the higher the product purity required, the lower the throughput. If product purity and yield are fixed, the larger the solute migration speed ratio, the higher the throughput, and the lower the desorbent consumption. If total bed volume and product purities are fixed, the longer the separation zones, the higher the throughput, but the higher the desorbent flow-rate. An intermediate configuration gives the minimum desorbent consumption. If there are no limits on pressure drop or zone flow-rate, the larger the column length to diameter ratio, the smaller the adsorbent particle size, the higher the throughput, and the lower the desorbent consumption. If the maximum zone flow-rate is controlled by the pressure drop limit and not by the standing waves requirement, the longer the columns, the lower the zone flow-rates and the lower the throughput. For 150-μm adsorbent particles and a maximum zone flow-rate of 300 ml/min, a design with optimal throughput and desorbent consumption is found for paclitaxel purification.

Keywords: Simulated moving bed; Optimization; Paclitaxel

1. Introduction

Most of the existing simulated moving-bed (SMB) systems have a four-zone configuration with two inlet ports (feed and desorbent) and two outlet ports (raffinate and extract) as shown in Fig. 1a. The four ports move periodically along the fluid flow direction to follow the two migrating solute bands. In this way, feed is always added in the region where the two bands overlap, whereas the two products are drawn from the regions where the bands do not overlap. In such a configuration, SMB chromatography has the advantages of recycle chromatography, which has high product purity, high yield, and low desorbent requirement [1]. It also has the advantages of a carousel process, which has a high adsorbent utilization and low labor cost [2].

SMB chromatography has been widely used for various industrial applications, such as hydrocarbon and sugar purification. All industrial-scale SMBs for hydrocarbon and high fructose corn syrup are low-pressure systems which employ large adsorbent

*Corresponding author.

0021-9673/99/$ – see front matter
PII: S0021-9673(99)00630-5

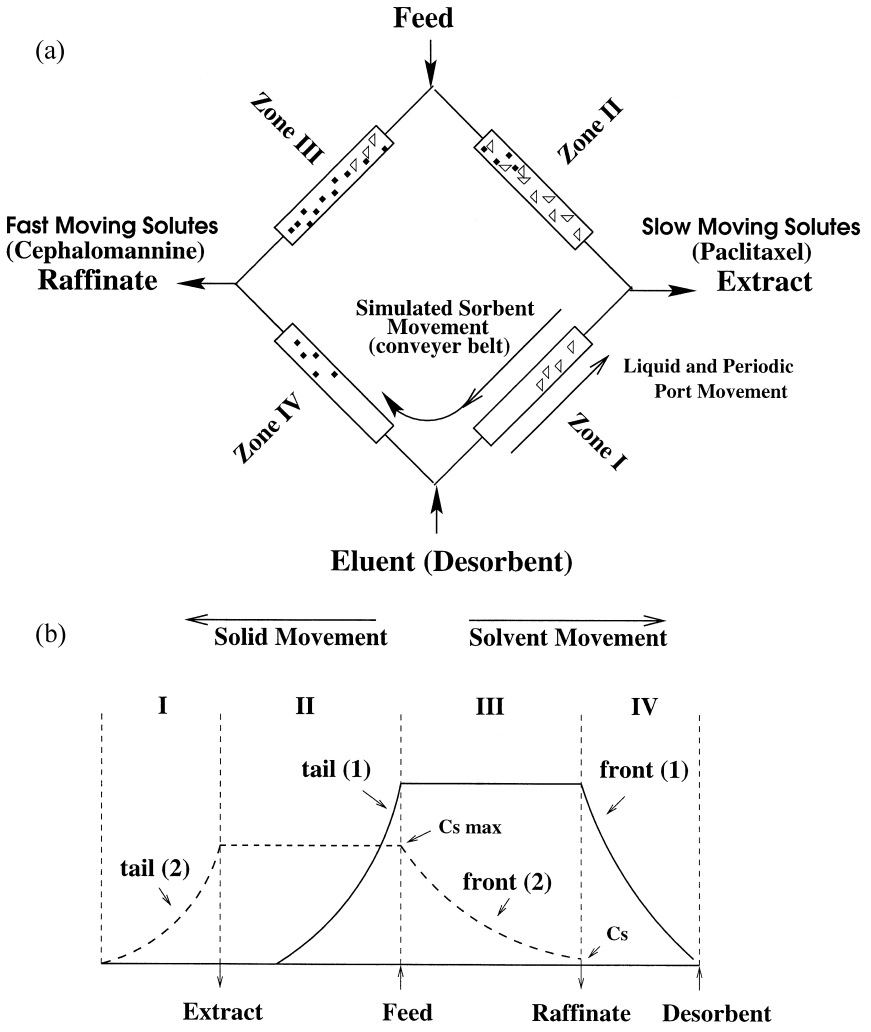

Fig. 1. (a) Schematic diagram of a four-zone SMB system. (b) Standing waves in linear CMB systems.

particles (600–1000 μm in diameter). These low-pressure SMBs have been proven to be economical for the commodity chemicals [3]. The goal of this study is to explore the design and optimization issues of low-pressure SMBs for the purification of an anti-cancer agent.

A successful SMB design depends on the selection of proper flow-rates in the four zones and the average port movement velocity (or port switching time) to achieve high product purity and high yield. In the literature, the zone flow-rates and port switching time in SMB are usually derived from the equilibrium theory, which cannot guarantee desired product purity for systems with mass-transfer effects [4–13]. The search of the design parameters that guarantee desired product purity requires trial and error, which is time consuming especially for systems with small separation factors and high purity requirements.

In a recent study by Ma and Wang [14], a standing wave analysis is developed for the design of continuous moving-bed (CMB) and SMB systems with linear isotherms. The analysis is based on the idea that there should be one standing concentration wave in each zone to ensure product purities (Fig. 1b). By proper selection of the four zone flow-rates and solid

movement velocity in CMB, the desorption wave of the slow moving solute can be 'standing' in zone I and its adsorption wave standing in zone III, while the desorption wave of the fast moving solute is 'standing' in zone II and its adsorption wave standing in zone IV (Fig. 1b). A similar strategy can be applied to SMB systems to achieve waves that are standing in a time averaged sense. Zones I and IV are used to achieve adsorbent regeneration and to prevent cross contamination and they are called the buffer zones. Zones II and III are used to achieve separation and they are called the separation zones. Under the standing wave condition, a set of simple algebraic equations have been derived to link product purity and recovery to zone lengths, solid movement velocity in CMB (or port switching time in SMB), zone flow-rates, isotherms, and mass-transfer parameters. The equations are used in this study to design and optimize a low-pressure pilot-scale SMB system for paclitaxel purification.

Paclitaxel is a promising anti-cancer agent and has been approved by the US Food and Drug Administration (FDA) for treating advanced breast cancer and refractory ovarian cancer. It also shows promise for the treatment of several other forms of cancer [15,16]. Paclitaxel separation and purification usually involves extraction, solvent partitioning, and preparative HPLC purification [17–21]. To eliminate the hazardous solvents and the expense associated with high-pressure equipment, Wu et al. [1] developed a low-pressure liquid chromatography (LPLC) process using a polymeric adsorbent and environmentally benign solvents — ethanol and water. This process can achieve high paclitaxel purity and yield from plant tissue culture broth. An economic analysis done by Wu et al. [1] shows that desorbent consumption contributes to a major fraction of the process cost. A more efficient process, SMB chromatography, is elected in this study to increase throughput and reduce desorbent consumption. A detailed comparison between SMB and batch-elution chromatography can be found elsewhere [22].

In many paclitaxel sources, cephalomannine is the closest eluting impurity. Below their solubilities in ethanol–water solutions, both paclitaxel and cephalomannine isotherms are linear for the adsorbent and solvents studied previously [1]. Therefore, the standing wave analysis for linear systems can be used to design and optimize SMB systems for the separation of paclitaxel from cephalomannine. A pilot-scale SMB system is selected in this study. The results show that maximum throughput or minimum desorbent consumption can be achieved by choosing an appropriate desorbent composition, column configuration (number of column in each zone), column length to diameter ratio, and adsorbent particle size. The effects of zone flow-rate and pressure drop constraints are also discussed.

2. Theory — standing wave design and optimization

The standing wave analysis for SMB systems with linear isotherms has been developed and the designs based on this analysis have been validated with data on sugar separations [14] and amino acid separations [23]. Here we give only a brief description of this analysis with emphasis on its application to SMB optimization.

2.1. Design equations under standing wave conditions

To achieve the four standing waves required for high purity and high yield, the flow-rates in the four zones must satisfy the following equations [14]:

$$(1+P\delta_2)\nu - u_0^{\mathrm{I}} = -\beta_2^{\mathrm{I}}\left(\frac{E_{b2}^{\mathrm{I}}}{L^{\mathrm{I}}} + \frac{P\nu^2\delta_2^2}{K_{f2}^{\mathrm{I}}L^{\mathrm{I}}}\right) \quad (1)$$

$$(1+P\delta_1)\nu - u_0^{\mathrm{II}} = -\beta_1^{\mathrm{II}}\left(\frac{E_{b1}^{\mathrm{II}}}{L^{\mathrm{II}}} + \frac{P\nu^2\delta_1^2}{K_{f1}^{\mathrm{II}}L^{\mathrm{II}}}\right) \quad (2)$$

$$(1+P\delta_2)\nu - u_0^{\mathrm{III}} = \beta_2^{\mathrm{III}}\left(\frac{E_{b2}^{\mathrm{III}}}{L^{\mathrm{III}}} + \frac{P\nu^2\delta_2^2}{K_{f2}^{\mathrm{III}}L^{\mathrm{III}}}\right) \quad (3)$$

$$(1+P\delta_1)\nu - u_0^{\mathrm{IV}} = \beta_1^{\mathrm{IV}}\left(\frac{E_{b1}^{\mathrm{IV}}}{L^{\mathrm{IV}}} + \frac{P\nu^2\delta_1^2}{K_{f1}^{\mathrm{IV}}L^{\mathrm{IV}}}\right) \quad (4)$$

$$\frac{F^{\mathrm{feed}}}{\epsilon_b S} = u_0^{\mathrm{III}} - u_0^{\mathrm{II}} \quad (5)$$

$$\frac{F^{\mathrm{des}}}{\epsilon_b S} = u_0^{\mathrm{I}} - u_0^{\mathrm{IV}} \quad (6)$$

Here u_0 is the interstitial velocity, $u \geq 0$ is the port movement velocity in the direction opposite to the desorbent flow, L is the zone length, S is the column cross sectional area, E_b is the axial dispersion coefficient, K_f is the lumped mass-transfer coefficient, $\delta_i \equiv \epsilon_p + (1-\epsilon_p)a_i$ (a_i is the partition constant between the adsorbed phase and the liquid phase for solute i), $P \equiv (1-\epsilon_b)/\epsilon_b$ is the bed phase ratio, ϵ_b is the interparticle void fraction, and ϵ_p is the intraparticle void fraction. β is related to the ratio of the highest concentration to the lowest concentration of the standing wave in the specified zone [14]. β_2^{III}, for example, is the natural logarithm of the ratio of the concentration at the inlet of zone III (C_{smax}) to that at the raffinate port (C_s) for solute 2 (Fig. 1b). It is used as an index of product purity and yield. The higher the β_2^{III} value, the higher the product purity of solute 1 in the raffinate and the higher the yield of solute 2 in the extract. To achieve high purity of solute 2 in the extract and high yield of solute 1 in the raffinate requires a high β_1^{II} value. Therefore, to ensure high purity and high yield of both solutes, a value of 5.5 is chosen for both β_2^{III} and β_1^{II} unless noted otherwise.

For a given feed flow-rate (F^{feed}), the average port movement velocity can be derived from Eqs. (2, 3 and 5) as

$$\left(\frac{P\beta_2^{III}\delta_2^2}{K_{f2}^{III}L^{III}} + \frac{P\beta_1^{II}\delta_1^2}{K_{f1}^{II}L^{II}}\right)\nu^2 - P(\delta_2-\delta_1)\nu + \frac{F^{feed}}{\epsilon_b S} + \frac{\beta_2^{III}E_{b2}^{III}}{L^{III}} + \frac{\beta_1^{II}E_{b1}^{II}}{L^{II}} = 0 \quad (7)$$

Similarly, if a desorbent flow-rate is given, ν can be derived from Eqs. (1, 4 and 6) as:

$$\left(\frac{P\beta_1^{IV}\delta_1^2}{K_{f1}^{IV}L^{IV}} + \frac{P\beta_2^{I}\delta_2^2}{K_{f2}^{I}L^{I}}\right)\nu^2 + P(\delta_2-\delta_1)\nu - \frac{F^{des}}{\epsilon_b S} + \frac{\beta_1^{IV}E_{b1}^{IV}}{L^{IV}} + \frac{\beta_2^{I}E_{b2}^{I}}{L^{I}} = 0 \quad (8)$$

If the product purities and the feed flow-rate are given, there are four equations (Eqs. (1–4)) to solve for four unknowns (three zone linear velocities and the port movement velocity). These equations determine the minimum linear velocities for zones I and II and the maximum linear velocities for zones III and IV. Any higher velocities in zones I and II or lower velocities in zones III and IV result in higher-than-required product purity and yield. However, product concentrations will be lower and solvent consumption will be higher. The equations also determine the minimum desorbent flow-rate (the flow-rate difference between zones I and IV) for the given purities and feed flow-rate.

When $\beta_1^{II} = \beta_2^{III} = \beta$, $K_{f1}^{II} = K_{f2}^{III} = K_f$, $E_{b1}^{II} = E_{b2}^{III} = E_b$, and $L^{II} = L^{III}$, the ν value solved from Eq. (7) should be a real number in order to have a physically meaning. Therefore, the following condition must be satisfied:

$$P(\alpha-1)^2 - 4\beta\left(\frac{\alpha^2+1}{K_f}\right)\left(\frac{F^{feed}}{\epsilon_b SL} + \frac{2\beta E_b}{L^2}\right) \geq 0 \quad (9)$$

where $\alpha(\equiv \delta_2/\delta_1)$ is the modified capacity ratio, which is related to both capacity and selectivity. For a given β, the maximum feed flow-rate can be found by letting the left-hand-side of Eq. (9) be zero. Eq. (9) links feed flow-rate to various system and operating parameters, such as zone lengths (L), axial dispersion coefficient (E_b), mass-transfer coefficient (K_f), and the α value.

The steady state effluent concentrations in CMB systems do not change with time. By contrast, the steady state effluent concentrations in SMB systems are cyclic if the adsorption wave of the fast moving solute passes through the raffinate port or the desorption wave of the slow moving solute passes through the extract port. SMB performance approaches that of CMB as the column number increases. As discussed in a previous paper, the time-averaged product concentrations (over one cycle) in a low-pressure SMB with eight columns or more are close to the concentrations in a corresponding CMB [14]. For such systems, the equations derived for CMB systems can be applied to SMB systems.

2.2. Numerical simulations

Numerical simulations of SMB chromatography based on a lumped mass-transfer model have been benchmarked with analytical solutions and experimental data for sugar separations [14]; they are used here for the cases where the flow-rate effects on

axial dispersion (E_b) and lumped mass-transfer coefficient (K_f) are considered. The E_b values can be estimated from the Chung and Wen correlation [24]. In linear systems, the K_f values can be found from the following equation [14]:

$$\frac{1}{K_f} = \frac{R^2}{15\epsilon_p D_p} + \frac{R}{3k_f} \tag{10}$$

where k_f is the film mass-transfer coefficient, which is estimated from the Wilson and Geankoplis correlation [25], and D_p is the effective pore diffusivity, which has been estimated from pulse and stepwise elution experiments [1,26].

2.3. Optimization strategies

2.3.1. Objectives

For the comparison of various SMB designs, a set of performance parameters needs to be defined. In many SMB applications, especially in the pharmaceutical industry, product purity and recovery are usually the most important factors. For the slow moving solute (solute 2), for example, product purity is related to the β_1^{II} value as follows

$$\text{purity}\% \equiv \frac{C_2^{ext}}{C_1^{ext} + C_2^{ext}} \cdot 100\% \simeq \frac{\exp(\beta_1^{II})}{\exp(\beta_1^{II}) + C_1^{III}/C_2^{III}} \cdot 100\% \tag{11}$$

where C_1^{ext} and C_2^{ext} are the concentrations at the extract port for solute 1 and solute 2, respectively. C^{III} is the solute concentration at the inlet of zone III, which can be different from the feed concentration because the feed is diluted by the stream from zone II. The concentration of solute 1 at the raffinate port is assumed to be the same as that at the inlet to zone III (C_1^{III}) (zone III is almost saturated). The concentration ratio of the two solutes at the inlet of zone III (C_1^{III}/C_2^{III}) is assumed to be the same as the ratio in the feed. If the solutes have the same feed concentrations and $\beta_1^{II} = \beta_2^{III}$, the purity should be the same for both solutes.

If product purity and yield are specified, one can maximize throughput and minimize desorbent consumption by changing system and operating parameters. Throughput in this study is defined as the amount of feed processed per unit volume of adsorbent per unit time, and desorbent consumption is defined as the amount of desorbent used to treat a unit weight of solute in the feed. They are determined from the following equations:

$$\text{Throughput} = \frac{F^{feed}}{BV} \tag{12}$$

$$\text{Desorbent consumption} \equiv \frac{F^{des}}{F^{feed} C_i^0} = \frac{\gamma}{C_i^0} \tag{13}$$

where BV is the total bed volume, C_i^0 is the concentration of solute i (the product) in the feed, γ is the ratio of desorbent flow-rate to feed flow-rate. In this study, both the total bed volume and the feed composition remain constant. Therefore, feed flow-rate is directly proportional to throughput (Eq. (12)) and the γ value is directly proportional to desorbent consumption (Eq. (13)). For the sake of simplicity, throughput and feed flow-rate are used interchangeably as are desorbent consumption and γ value.

When column dimensions and zone lengths are fixed, the higher the product purity the lower the feed flow-rate; the theoretical maximum β can be found from Eq. (9) when feed input is zero. If the maximum β is larger than the required β (which can be found from the required product purity), the system can then be optimized in terms of throughput and desorbent consumption. If the required product purity results in β value that exceeds the theoretical maximum β, the system needs a new configuration, longer columns, a new adsorbent, or a new desorbent. If product purity and yield are specified, there is a maximum feed flow-rate for a given system according to Eq. (9). From now on, feed flow-rate means the maximum feed flow-rate calculated from this equation unless noted otherwise. For each feed flow-rate, ν is calculated from Eq. (7) and a desorbent flow-rate is then calculated from Eq. (8). According to the standing wave analysis, this desorbent flow-rate is minimum for the given feed flow-rate. Below, desorbent flow-rate means the minimum desorbent flow-rate calculated from Eq. (8) unless noted otherwise. If E_b and K_f do not change with flow-rates, the feed and desorbent flow-rates can be directly calculated from Eqs. (1–6).

2.3.2. Constraints

In practice, a low-pressure SMB apparatus has a zone flow-rate constraint or a pressure drop limit, which is determined by the pump capacity, adsorbent particle size, or column length. Under such a constraint, the feed flow-rate from Eq. (9) may not be allowed by the system. Therefore, the feed flow-rate can be limited by the equipment, not by the theoretical values obtained from the standing wave analysis, Eq. (9).

Paclitaxel purification is used below as an example to show how desorbent composition, column configuration, column geometry, and adsorbent particle size affect throughput and desorbent consumption with or without a zone flow-rate constraint or a pressure drop limit.

3. Paclitaxel system

A comprehensive experimental study of low-pressure batch and recycle chromatography has been reported on the separation of paclitaxel and cephalomannine using a high capacity polystyrene–divinylbenzene adsorbent (DOW LSR-62-26A) and a mobile phase of ethanol and water [1,26]. The adsorbent was from Dow (Midland, MI, USA) and the smallest particle size that was commercially available at that time was about 150 μm in diameter. For a solution with 40% ethanol (v/v), the paclitaxel solubility is more than 150 mg/l. In pure ethanol, its solubility is about 10 g/l. In the systems studied here, both paclitaxel and cephalomannine isotherms are linear with respect to their concentrations. The effects of ethanol concentration on the isotherms are correlated by the following linear reversed-phase modulator equations

$$Q_{\text{Paclitaxel}} = 2852.3 \cdot \exp(-5.3757\phi) C_{\text{Paclitaxel}} \quad (14)$$

$$Q_{\text{Cephalomannine}} = 2150.3 \cdot \exp(-5.4184\phi) C_{\text{Cephalomannine}} \quad (15)$$

Here Q has the units of mg per ml solid adsorbent, and ϕ is the ethanol concentration in the desorbent.

Paclitaxel has a higher affinity than cephalomannine over the ethanol concentration range from 40 to 100%. Paclitaxel, the desired product, is designated as solute 2 (slow moving solute) while cephalomannine as solute 1 (fast moving solute). In a four-zone SMB system (Fig. 1a), paclitaxel is recovered in the extract and cephalomannine in the raffinate.

A typical commercial pilot-scale SMB system, the CSEP Model C920 from AST (Lakeland, FL, USA), is chosen as a benchmark case. The zone flow-rates and pressure drop limit are similar to those of the Mini-ADSEP pilot-scale SMB from US Filter (Rockford, IL, USA). The system has 20 columns, 55×7.5 cm I.D. for each column. The maximum allowed zone flow-rate for this SMB system is 300 ml/min. Unless noted otherwise, column configuration is set to be 3-7-7-3, which means there are 3, 7, 7 and 3 columns in zones I, II, III and IV, respectively; adsorbent particle size is 300 μm in diameter, which is a typical size of a low-pressure polymeric adsorbent; desorbent composition is 80% ethanol in water; and both paclitaxel and cephalomannine concentrations in the feed are 150 mg/l, which is a reported paclitaxel concentration in a plant tissue culture broth [27]. Other parameters are listed in Table 1.

4. Results and discussion

4.1. Maximum allowed purity and tradeoff between throughput and product purity

As expected from Eq. (9), the β value reaches its theoretical maximum if there is no feed flow. For the given equipment and system parameters in Table 1, the maximum β value is 50.6, which is much larger than the required value of $\beta = 5.5$ (corresponding to 99.6% paclitaxel purity). At the required purity, the maximum possible feed flow-rate from Eq. (9) is 98.4 ml/min. The throughput is 6.7 l feed/l adsorbent/day and the desorbent consumption is 30.3 l desorbent/g paclitaxel in feed. The standing wave analysis shows that the throughput and desorbent consumption in this system are functions of desired paclitaxel purity as shown in Fig. 2. The E_b and K_f values in Eqs. (1–4) are assumed to be constants and they do not change with flow-rates. There is a tradeoff between throughput and paclitaxel purity. A lower throughput results in a higher paclitaxel purity and vice versa. At a lower feed flow-rate (through-

Table 1
Design parameters for the benchmark SMB system (Design I)

Zone	Zone I	Zone II	Zone III	Zone IV
Column no.	3	7	7	3
Length (cm)	165	385	385	165
Single column	R (μm) 150	L (cm) 55	$\epsilon_p(\epsilon_b)$ 0.753 (0.433)	I.D. (cm) 7.5
Isotherm constants	$a_{\text{paclitaxel}}$ (80%) 38.68	$a_{\text{cephalomannine}}$ (80%) 28.18		
Mass-transfer	E_b (cm^2/min) 2.1596	k_f (cm/min) 0.1995	D_p (cm^2/min) 1.31e-04	K_f (1/min) 5.650
Feed (mg/l)	$C^0_{\text{cephalomannine}}$ 150	$C^0_{\text{paclitaxel}}$ 150		

put), the two solute bands are better separated, and therefore a higher purity is obtained. However, a higher purity requires more desorbent, especially when purity is higher than 98%. The curves in Fig. 2 define the boundaries between feasible designs and unfeasible designs. The regions below the throughput curve and above the desorbent consumption curve are feasible, which means the required product purity can be achieved when the SMB system is operated at a lower feed flow-rate or a higher desorbent flow-rate than those for the standing wave designs. The standing wave designs (the curve values) therefore give the maximum throughput and the minimum desorbent consumption for the given purity requirement and the given SMB equipment.

The throughput at a given product purity is affected by various design parameters. In the following analysis, the choices of desorbent composition, column configuration, column geometry, and adsorbent particle size are studied for their effects on throughput and desorbent consumption at 99.6% product purities. For easy comparison, only one parameter is changed at a time and the rest are kept the same as those in Table 1.

4.2. Choice of desorbent composition

The selection of desorbent composition is important for SMB throughput and desorbent consumption. As shown in this system, both affinity and

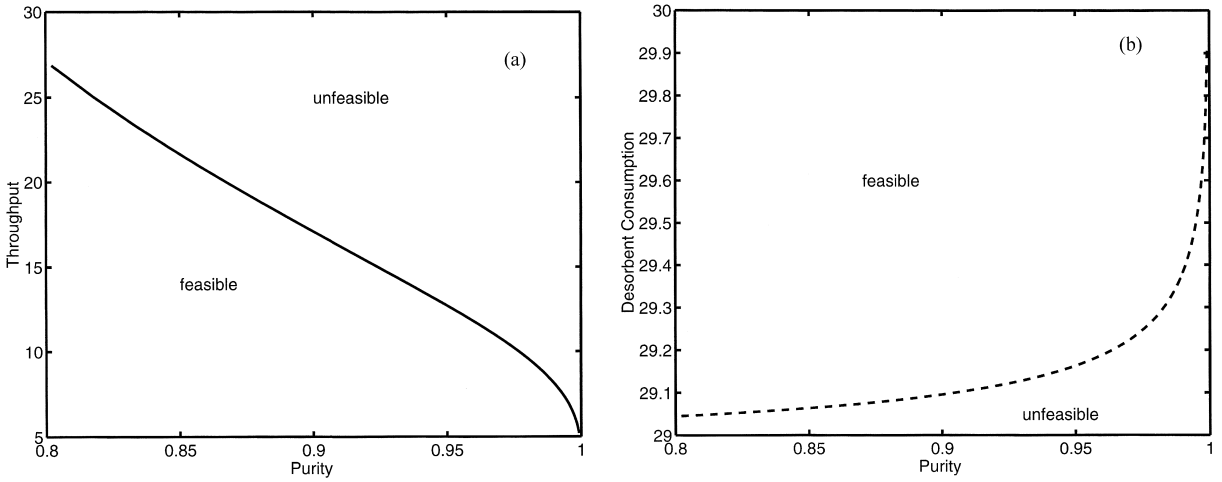

Fig. 2. (a) Relations between throughput and product purity. (b) Relations between desorbent consumption and product purity.

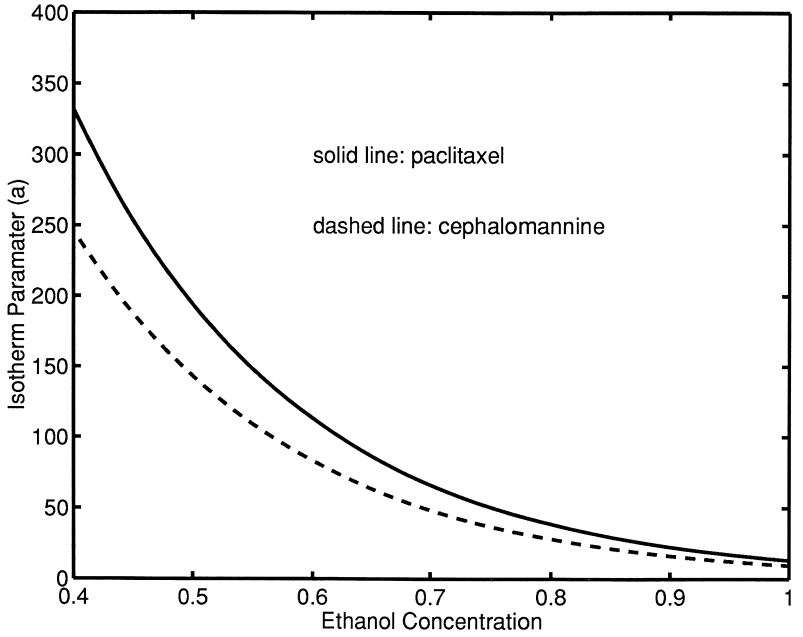

Fig. 3. Relation between isotherm constant (a) and ethanol fraction in mobile phase. Solid line is paclitaxel (solute 2) and dashed line is cephalomannine (solute 1).

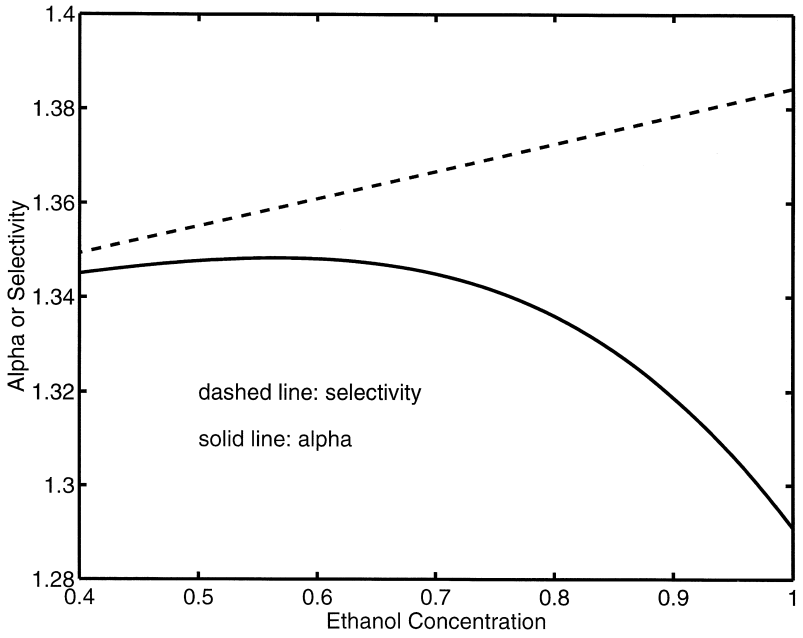

Fig. 4. Effects of ethanol concentration in desorbent on modified capacity factor ratio α and selectivity. α is defined as δ_2/δ_1 and selectivity is defined as $(a_{\text{paclitaxel}}/a_{\text{cephalomannine}})$.

selectivity vary with the ethanol concentration in the desorbent. Figs. 3 and 4 indicate that isotherm parameter a (affinity) and selectivity ($a_{\text{pacitaxel}}/a_{\text{cephalomannine}}$) vary in opposite directions as ethanol concentration increases. The higher the ethanol concentration, the lower the affinity (Fig. 3) and the higher the selectivity (Fig. 4). The ratio α ($\equiv \delta_2/\delta_1$, which corresponds to the solute migration speed ratio and is a function of $a_{\text{paclitaxel}}$, $a_{\text{cephalomannine}}$ and ϵ_p) shows a maximum value when the ethanol concentration is about 60% (Fig. 4). At this ethanol concentration, the feed flow-rate is the highest and the desorbent consumption is the lowest (Fig. 5). As expected from Eq. (9), the higher the α value (which is approximately the solute migration speed ratio), the higher the feed flow-rate. Similarly, Eq. (8) suggests that the higher the solute migration speed ratio the smaller the desorbent consumption. The highest solute migration speed ratio (at 60% ethanol in this case) gives the highest throughput and the lowest desorbent consumption.

The effects of α on throughput and desorbent consumption result from both affinity and selectivity. To study the effect of affinity separately, we change the isotherm parameters (a) and keep the selectivity the same. Fig. 6 indicates that a higher affinity (higher a value for paclitaxel) results in a higher throughput and a smaller γ. This figure also shows that for a selectivity of 1.37, little increase in throughput or decrease in desorbent consumption is gained when a is greater than 50. The effect of selectivity is studied separately by changing the isotherm parameter for cephalomannine, while the isotherm parameter for paclitaxel ($a_{\text{pacitaxel}}$) is kept the same (a value of 38.68 corresponds to 60% ethanol concentration in the desorbent). Fig. 7 shows that the larger the selectivity, the higher the throughput (or feed flow-rate), and the smaller the desorbent consumption (or γ). However, little improvement in throughput is gained when the selectivity is greater than 5 and little improvement is gained in desorbent consumption when the selectivity is greater than 2.0. As selectivity decreases to below 1.5, a sharp rise in desorbent consumption is observed.

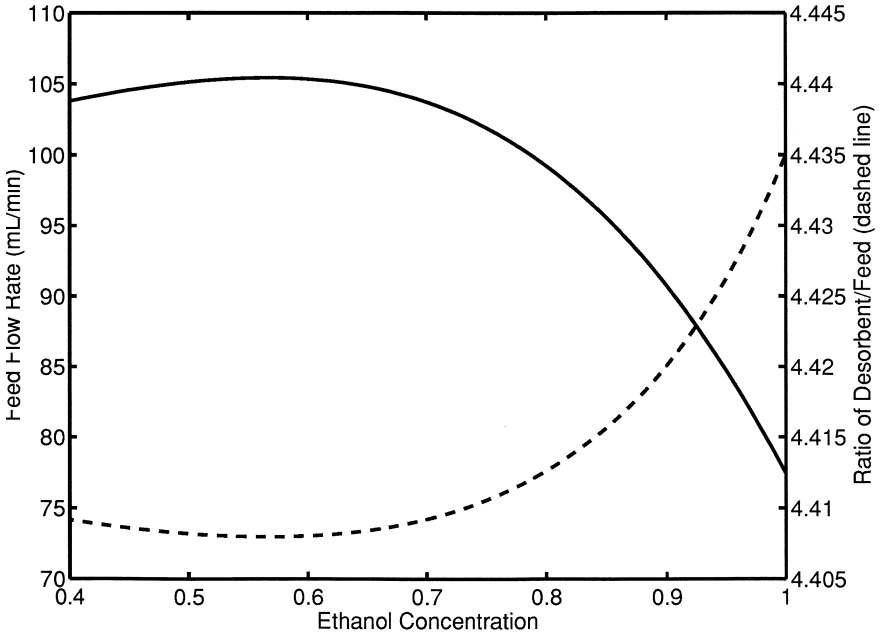

Fig. 5. Effects of ethanol concentration in desorbent on maximum feed flow-rate and γ (ratio of desorbent flow-rate to feed flow-rate) when the effect of flow-rates on K_f and E_b are neglected.

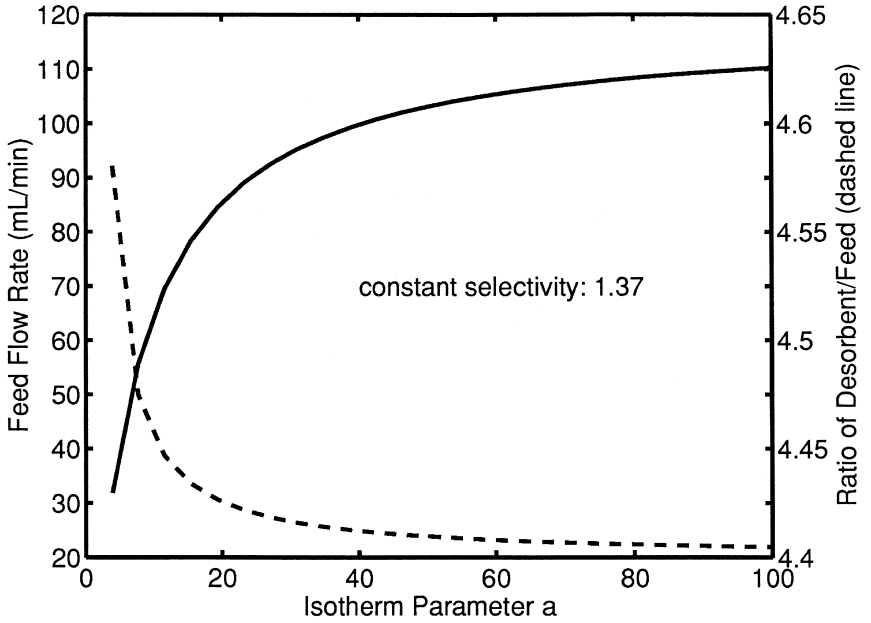

Fig. 6. Effects of isotherm parameter a on feed flow-rate and γ when selectivity is a constant (1.37) and the effect of flow-rates on K_f and E_b are neglected.

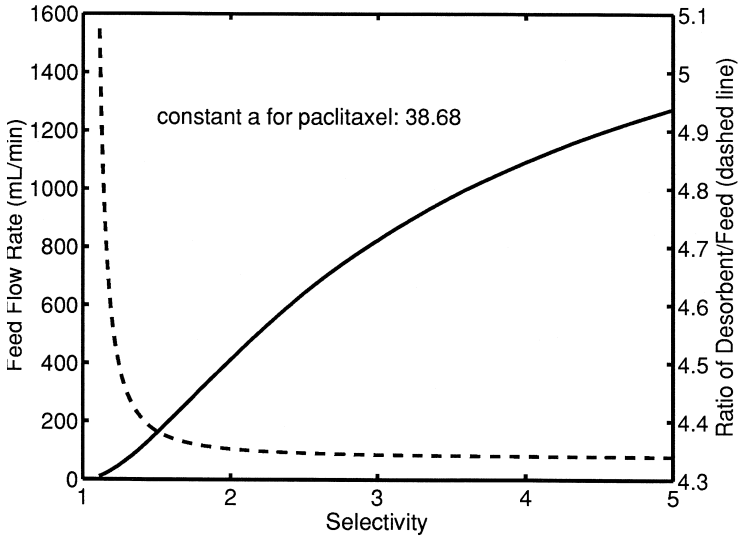

Fig. 7. Effects of selectivity on maximum feed flow-rate and γ when isotherm parameter a for paclitaxel is a constant (38.68) and the effect of flow-rates on K_f and E_b are neglected.

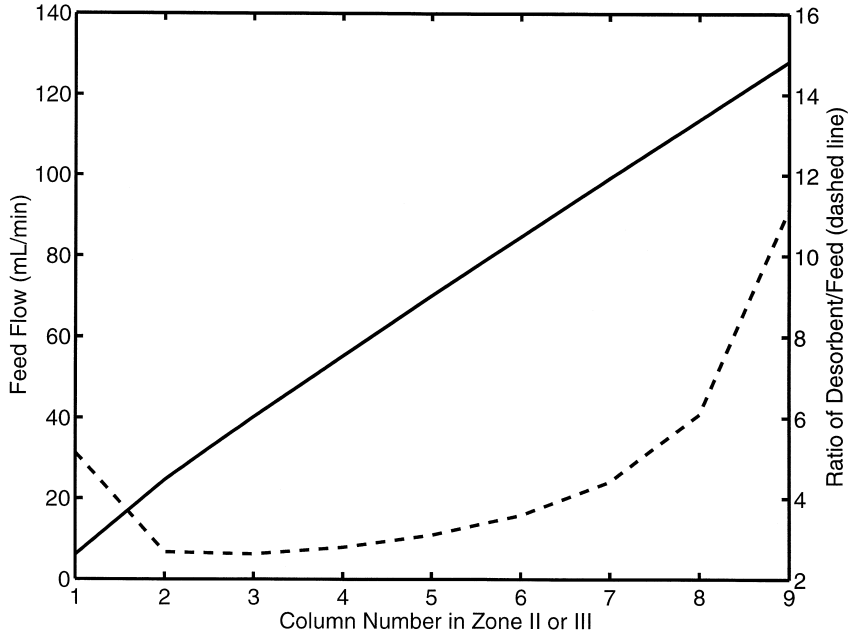

Fig. 8. Effects of column number in zones II or III (configuration) on maximum feed flow-rate and γ when the effect of flow-rates on K_f and E_b are neglected.

4.3. Effect of column configuration

If the total bed volume and column dimension are fixed, the longer the separation zones (zones II and III), the shorter the buffer zones (zones I and IV). In this study, zones I and IV have the same number of columns, so do zones II and III. If the column number in the separation zones increases, the two solute bands will be better separated because of the longer zone length. If both paclitaxel and cephalomannine purities are fixed (99.6%), more feed can be loaded and the feed flow-rate (throughput) increases as the length of the separation zones increases (Fig. 8). However, a higher desorbent flow-rate is needed to prevent cross contamination because the buffer zones are shorter. If maximal throughput is the only objective, configuration 1-9-9-1 should be selected. Even though the desorbent flow-rate is minimum at configuration 9-1-1-9, the ratio of desorbent flow-rate to feed flow-rate (desorbent consumption) shows a minimum for the 8-2-2-8 configuration. If minimal desorbent consumption is the only objective, the configuration 8-2-2-8 should be the choice.

4.4. Effects of column geometry

If total bed volume and column configuration are kept constant, an increase in column length results in a decrease in column diameter. Increasing column length improves separation. Therefore, a higher feed flow-rate and a lower desorbent flow-rate are obtained when the column length to diameter ratio increases (Fig. 9). If the column length to diameter ratio is greater than 7.3, there is no significant improvement in both throughput (feed flow-rate) and desorbent consumption (ratio of desorbent to feed flow-rate).

4.5. Effects of adsorbent particle size

Although there is no explicit dependence on particle size in the design equations, adsorbent particle size is an important parameter because it can significantly affect the lumped mass-transfer coefficient K_f (Eq. (10)) and the axial dispersion coefficient E_b. A smaller particle size results in a larger K_f, a smaller E_b, and sharper waves. For a given total

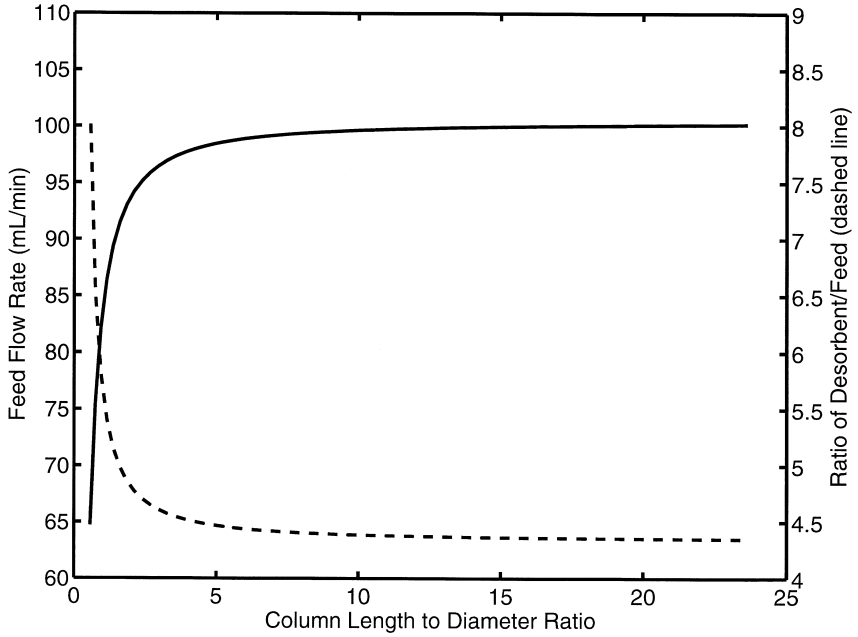

Fig. 9. Effects of column length in zones II or III (column geometry) on maximum feed flow-rate and γ when the effect of flow-rates on K_f and E_b are neglected.

bed volume and product purities, the feed flow-rate can be higher when a smaller particle size is used (Fig. 10). A wide range of adsorbent particle sizes can meet the high purity requirement using the standing wave design because the impurity waves are kept away from the product ports. However, the waves are more spread for a large particle system. As a result, a lower feed flow-rate (or throughput) is required to achieve the same purity as in a small particle system. Fig. 10 also shows that the desorbent consumption decreases with decreasing adsorbent particle size. Therefore, a smaller adsorbent particle size gives a higher throughput with a lower desorbent consumption.

In the above analysis (Sections 4.1–4.5), we assume that E_b and K_f do not change with the flow-rates and there is no zone flow-rate or pressure drop constraint. Each zone flow-rate and the switching time can be directly solved from Eqs. (1–5). However, if the effects of flow-rates on E_b and K_f are considered and the zone flow-rate is limited to 300 ml/min, iterations are needed to solve zone flow-rates and switching time from the design equations. Simulations based on a lumped model [14] are used to find the effects of the four design parameters (desorbent composition, column configuration, column geometry, and desorbent particle size) on throughput and desorbent consumption. Under a zone flow-rate limit of 300 ml/min, simulation results show that the design parameters have less significant effects on throughput and desorbent consumption than those shown in Figs. 5 and 8–10.

In practice, in addition to the zone flow-rate constraint, pressure drop constraint may also need to be considered. The maximum allowed pressure drop (ΔP) for low-pressure SMBs that are commercially available is about 100 p.s.i. Since this study focuses on low-pressure SMB systems, a pressure drop of 100 p.s.i. is used here as the limit. The product purity (99.6%), the column configuration (3-7-7-3), and the total bed volume (BV) are kept constant in the analysis. The pressure drop can be estimated from the Blake–Kozeny equation for laminar flow, which relates ΔP to adsorbent particle size ($2R$, R is adsorbent particle radius), zone length (L) and zone flow-rate (F_{max})

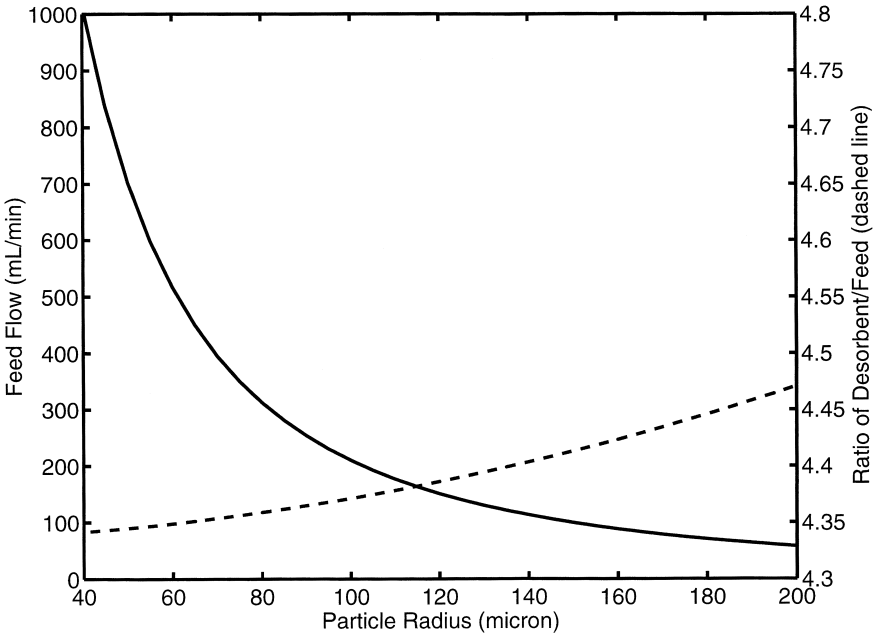

Fig. 10. Effects of adsorbent particle size on maximum feed flow-rate and γ when the effect of flow-rates on K_f and E_b are neglected.

$$\Delta P = \frac{37.5\mu F_{max} L(1-\epsilon_b)^2}{SR^2\epsilon_b^3} \quad (16)$$

where S is the column cross-sectional area. For a given adsorbent particle size, to keep the same pressure drop (100 p.s.i.), there can be different combinations between maximum allowed zone length (L) and the maximum allowed zone flow-rate (F_{max}). The throughput (feed flow-rate) and desorbent consumption (ratio of desorbent and feed flow-rates) for each combination can be found from the standing wave design equations. The results for three different adsorbent particle sizes (300, 150 and 60 μm in diameter) are shown in Fig. 11a and b.

When the adsorbent particle size is 300 μm, all the F_{max} values for 0.06 to 20.75 column length to diameter ratios (2.2 to 110 cm in column length) are larger than the corresponding zone I flow-rates calculated from the standing wave design equations. Zone I has the highest flow-rate among the four zones. This result indicates that the pressure drop limit has no effect on the SMB operation when the adsorbent particle size is 300 μm. As shown in Fig. 11, the larger the column length to diameter ratio, the higher the throughput and the lower the desorbent consumption. But the change of desorbent consumption with column length is small.

For the 150-μm adsorbent particle size, when the column length to diameter ratio is larger than 2.67 (28 cm in column length), the F_{max} values are smaller than the corresponding zone I flow-rates for the standing wave designs. To meet the ΔP limit, the larger the column length to diameter ratio, the lower the F_{max} value. Both the throughput and desorbent consumption decrease with increasing column length to diameter ratio (Fig. 11). By contrast, when the column length to diameter ratio is smaller than 2.67, the F_{max} values are larger than the standing wave zone I flow-rates. The throughput increases with increasing column length to diameter ratio (Fig. 11). When the column length to diameter ratio is 2.67, throughput reaches a maximum, which is 67.5 l feed/l adsorbent/day. The corresponding desorbent consumption is 29.0 l desorbent/g paclitaxel in feed.

When the adsorbent particle size is 60 μm, the changes of throughput and desorbent consumption with column length to diameter ratio have similar trends as those when the adsorbent particle size is

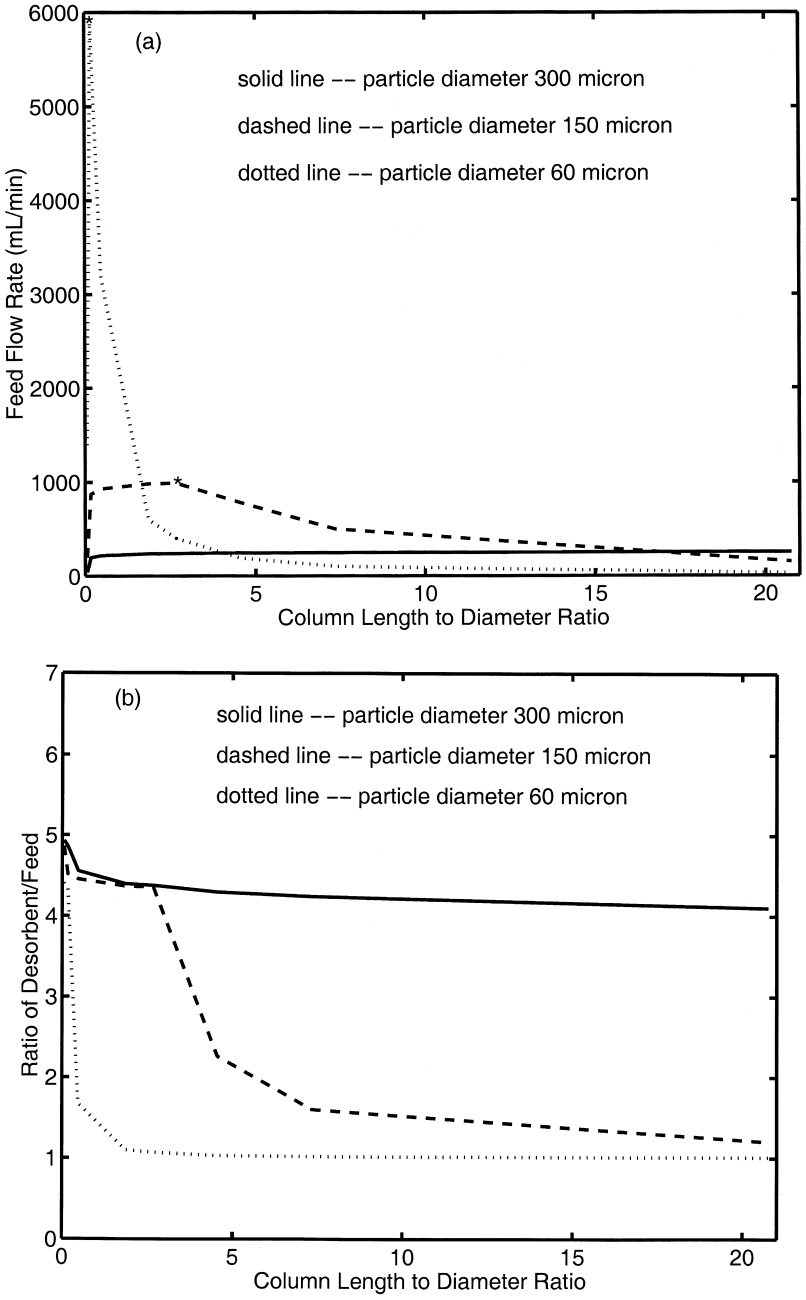

Fig. 11. Effects of adsorbent particle size and column length to diameter ratio on (a) maximum feed flow-rate and (b) γ under a pressure drop limit of 100 p.s.i.a. The point marked by * indicates the optimal column length to diameter ratio for a given adsorbent particle size where the controlling factor for zone I flow-rate changes from standing wave control to pressure drop control.

150 μm (Fig. 11). At this adsorbent particle size, throughput reaches a maximum when the column length to diameter ratio is 0.17 (4.4 cm in column length) instead of 2.67.

In general, when the pressure drop constraint allows the use of the zone flow-rates calculated from the standing wave design equations, the larger the column length to diameter ratio, the higher the throughput and the lower desorbent consumption. However, if F_{max} values based on the pressure drop limit are smaller than the calculated zone flow-rates based on the standing wave design, then a larger column length to diameter ratio results in a lower throughput. Maximum throughput is achieved at the optimal column length to diameter ratio where the controlling factor for the flow-rate in zone I changes from standing wave control to pressure drop control. Smaller particles give a higher throughput and a lower desorbent consumption when the column length to diameter ratio is optimal.

4.6. Selected design for a given adsorbent particle size and a zone flow-rate limit

In the above analysis, there is only one parameter changed at a time. All parameters need to be studied before finding an optimal design for paclitaxel purification. First, we need to define the ranges for the parameters. As mentioned in Section 3, for the selected adsorbent, the smallest commercially available size is about 150 μm in diameter. The ethanol concentration in the desorbent can vary from 40 to 100% because of paclitaxel solubility. The corresponding range of α is from 1.29 to 1.35. The total bed volume and the feed composition are kept constant. The maximum zone flow-rate is 300 ml/min. Here, throughput is assumed to be the primary consideration. In the defined ranges, ethanol concentration 60% (maximum α), configuration 1-9-9-1, column length 55 cm, and adsorbent particle diameter 150 μm, are chosen as the initial design condition.

The ethanol concentration is first analyzed to maximize throughput by examining a series of throughput and α relation curves at different column configurations, column geometry, and adsorbent particle size. For all the curves, throughput reaches a maximum at 60% ethanol concentration. Therefore, this concentration is chosen and will be used as a constant in the analysis of column configuration, column geometry, and adsorbent particle size. Within the ranges of the design parameters, the condition with 150 μm adsorbent particle diameter, 60%

Table 2
Design and operating parameters for the selected SMB system under the constraint of 302 ml/min maximum zone flow-rate (Design II)

Zone no.	Zone I	Zone II	Zone III	Zone IV
Column no.	3	7	7	3
Length (cm)	165	385	385	165
Flow (ml/min)	302	191	294	188
Single column	R (μm) 75	L (cm) 55	$\epsilon_p(\epsilon_b)$ 0.753 (0.433)	I.D. (cm) 7.5
Isotherm constants	$a_{paclitaxel}$ (60%) 133.35	$a_{cephalomannine}$ (60%) 83.29		
Mass-transfer	E_b (cm^2/min) 0.4045	k_f (cm/min) 0.2855	D_p (cm^2/min) 1.31e04	K_f (l/min) 21.14
Feed (mg/l)	$C^0_{cephalomannine}$ 150	$C_{paclitaxel}$ 150		
Input/output (ml/min)	Feed 103.00	Desorbent 114.18	Raffinate 106.34	Extract 110.84
Other parameters	Switching (min) 159.53	Transient (min) 5000		

ethanol concentration, 55 cm column length, and 1-9-9-1 column configuration gives the highest throughput. In fact, if a smaller adsorbent particle size is available, it should be chosen to give a higher throughput.

For desorbent composition, column geometry, and adsorbent particle size, the condition that gives higher throughput also gives lower desorbent consumption. Therefore, only column configuration is considered here for the optimization of desorbent consumption. At the condition with 60% ethanol concentration, 55 cm column length, 150 μm adsorbent particle diameter, and 300 ml/min zone flow-rate limit, the desorbent consumption is the minimum at the configuration 3-7-7-3. Since throughput difference between the configurations 3-7-7-3 and 1-9-9-1 is insignificant, the configuration 3-7-7-3 is selected as the configuration for minimum desorbent consumption.

Based on the selected parameters (Table 2), the operation parameters and the transient time are obtained from the standing wave analysis. The column profile and the time-averaged (over one cycle) effluent histories are obtained from computer simulations and plotted as Fig. 12.

If different ranges of parameters or different operation constraints are used, designs should be different to ensure the maximal throughput or the

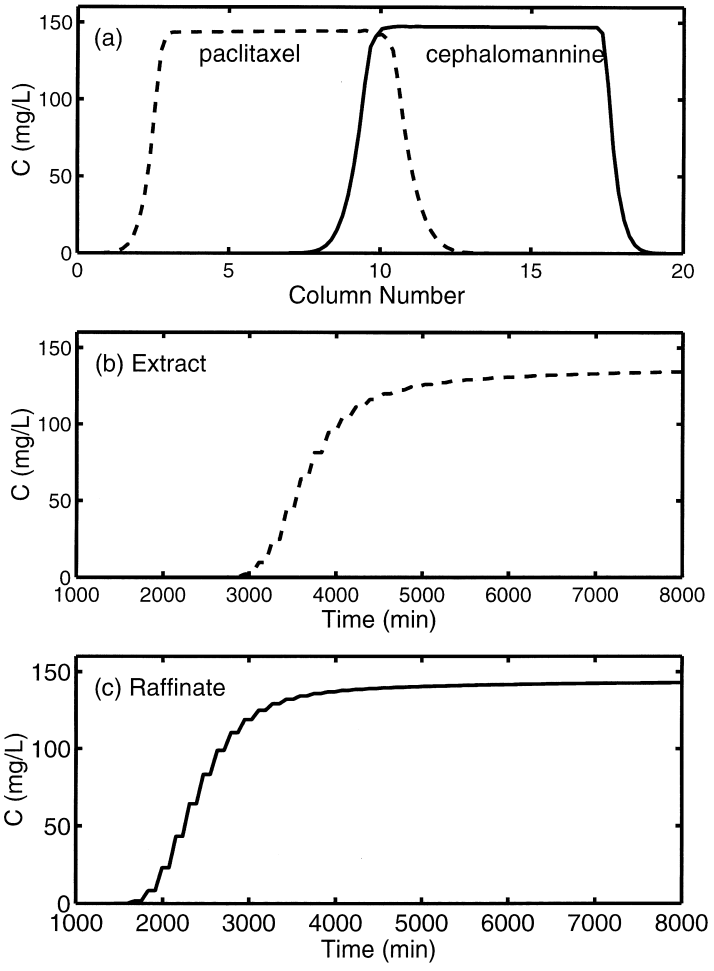

Fig. 12. Column concentration profile at the steady state and time-averaged effluent histories at the selected condition in Table 2.

Table 3
Comparison of throughput and desorbent consumption for SMB designs with different constraints

	Design I	Design II	Design III	Design IV
Constraint	None	300 ml/min F_{max}	100 p.s.i. ΔP	100 p.s.i. ΔP
Zone I ΔP (p.s.i.)	14	17	100	100
Desorbent (vol% ethanol)	80	60	60	60
Particle diameter (μm)	300	150	150	60
Column length (cm)	55	55	28	4.4
Column diameter (cm)	7.5	7.5	10.5	26.5
Throughput (l feed/l adsorbent/day)	6.7	7.1	67.5	403.3
Desorbent consumption (l desorbent/g paclitaxel)	30.3	7.4	29.0	28.9

minimal desorbent consumption. Table 3 compares four different designs with different adsorbent particle sizes or different constraints: the initial design for a typical SMB without zone flow-rate and pressure drop limits (Design I), the selected design with a zone flow-rate limit of 300 ml/min and an adsorbent particle diameter of 150 μm (Design II), the design with a pressure drop limit of 100 p.s.i.a. and an adsorbent particle diameter of 150 μm (Design III), and the design with a pressure drop limit of 100 p.s.i.a. and an adsorbent particle diameter of 60 μm (Design IV). For all the designs, column configuration (3-7-7-3), total bed volume, and purity requirement (99.6%) are kept the same. Even with the zone flow-rate constraint, Design II has a higher throughput and requires less desorbent than Design I. The comparison between Designs II and III shows that the design with a higher pressure drop limit has a higher throughput, but it also consumes more desorbent. Design IV shows that 60-μm adsorbent particle, if available, gives the highest throughput when the column length to diameter ratio is optimal. The throughput for the four designs are comparable or higher than the low-pressure SMBs for amino acid purification [23] and high fructose corn syrup purification [28].

5. Conclusions

For a typical low-pressure SMB unit, the higher the purity requirement, the lower the throughput and the higher the desorbent consumption. If product purity and yield are fixed, throughput and desorbent consumption are significantly affected by four major design parameters: desorbent composition, column configuration, column geometry (ratio of column length to diameter) and adsorbent particle size. The analysis shows that the higher the solute migration speed ratio, the higher the throughput, and the lower the desorbent consumption. Without either zone flow-rate or pressure drop limit, longer separation zones give a higher throughput, but longer buffer zones give a lower desorbent flow-rate. There is an intermediate configuration that gives the minimum desorbent consumption. When the total bed volume is kept constant, as the ratio of column length to diameter increases, throughput increases and desorbent consumption decreases. However, the change is less significant when the column length to diameter ratio exceeds 7.3. Adsorbent particle size significantly affects throughput and desorbent consumption. Smaller particles give a higher throughput and a lower desorbent consumption. However, column pressure drop increases with decreasing particle size.

If the maximum allowed flow-rates under a pressure drop limit are greater than the zone flow-rates calculated from the standing wave design equations, throughput increases and desorbent consumption decreases with increasing column length to diameter ratio. If the maximum zone flow-rate is controlled by the pressure drop limit and not by the standing wave requirement, the longer the column length to diam-

eter ratio, the lower the maximum allowed zone flow-rate, and the lower the throughput. In general, throughput reaches a maximal value at a critical column length to diameter ratio where the controlling factor of zone flow-rate changes from standing wave control to pressure drop control. When a pressure drop constraint exists, smaller adsorbent particles do not always achieve higher throughputs than larger adsorbent particles. This study shows that an optimal SMB design depends on the specific separation objectives and constraints. For a given adsorbent particle size of 150 μm and a zone flow-rate limit of 300 ml/min, an optimal design in terms of throughput and desorbent consumption is found for paclitaxel purification.

6. Notation

BV	total bed volume (ml)
C_i^0	solute i concentration in feed (mg/l)
C_i^{III}	solute i concentration at the inlet to zone III (mg/l)
C_i^{ext}	solute i concentration at the extract port (mg/l)
CMB	continuous moving bed
D_p	pore diffusion coefficient (cm^2/min)
E_b	axial dispersion coefficient (cm^2/min)
F^{feed}	feed volumetric flow-rate (ml/min)
F^{des}	desorbent volumetric flow-rate (ml/min)
F_{max}	maximum allowed zone flow-rate (ml/min)
HPLC	high-performance liquid chromatography
I.D.	inner diameter (cm)
K_f	lumped mass-transfer coefficient (l/min)
L	zone length (cm)
LPLC	low-pressure liquid chromatography
P	bed phase ratio $(1-\epsilon_b/\epsilon_b)$
R	adsorbent particle radius (μm)
S	column cross-section area (cm^2)
SMB	simulated moving bed
a	isotherm constant (per solid volume)
k_f	film mass-transfer coefficient (cm/min)
u_0	interstitial linear velocity (cm/min)
α	δ_2/δ_1 modified capacity ratio
β	logarithm of concentration ratio
γ	ratio of desorbent flow-rate to feed flow-rate
δ	$\epsilon_p + (1-\epsilon_p)a_i$
ϵ_b	interparticle void
ϵ_p	intraparticle porosity
ν	solid movement linear velocity (cm/min)
ϕ	volume fraction of solvent in desorbent

Acknowledgements

This research was supported by grants from NSF (GER9024174), Bristol-Myers Squibb Company, and the Purdue Research Foundation.

References

[1] D.-J. Wu, Z. Ma, B.W. Au, N.-H.L. Wang, AIChE J. 43 (1997) 232.
[2] M.V. Ernest Jr., J.P. Bibler, R.D. Whitley, N.-H.L. Wang, Ind. Eng. Chem. Res. 36 (1997) 2775.
[3] G. Parkinson, G. Ondrey, S. Mooy, Chem. Eng. 101 (1994) 30.
[4] L.S. Pais, J.W. Loureiro, A.E. Rodrigues, Chem. Eng. Sci. 52 (1997) 245.
[5] D.M. Ruthven, C.B. Ching, Chem. Eng. Sci. 44 (1989) 1011.
[6] S. Adachi, J. Chromatogr. A 658 (1994) 271.
[7] C.B. Ching, K.H. Chu, K. Hidajat, M.S. Uddin, AIChE J. 38 (1992) 1744.
[8] G. Storti, M. Masi, S. Carra, M. Morbidelli, Chem. Eng. Sci. 44 (1989) 1329.
[9] G. Storti, M. Mazzotti, M. Morbidelli, S. Carra, AIChE J. 39 (1993) 471.
[10] G. Storti, R. Baciocchi, M. Mazzotti, M. Morbidelli, Ind. Eng. Chem. Res. 34 (1995) 288.
[11] M.M. Hassan, K.F. Loughlin, M.E. Biswas, Sep. Technol. 6 (1996) 19.
[12] J. Strube, U. Altenhoner, M. Meurer, H. Schmidt-Tranb, M. Schulte, J. Chromatogr. A 769 (1997) 81.
[13] T. Yun, Z. Bensetiti, C. Zhong, O. Guiochon, J. Chromatogr. A 758 (1997) 175.
[14] Z. Ma, N.-H.L. Wang, AIChE J. 43 (1997) 2488.
[15] C. Joyce, BioScience 43 (1993) 133.
[16] M. Suffness (Ed.), TAXOL, Science and Applications, CRC Press, Boca Raton, FL, 1995.
[17] D.G.I. Kingston, D.R. Hawkins, L. Ovington, J. Nat. Products 45 (1982) 466.
[18] K.M. Witherup, S.A. Look, M.W. Stasko, T.J. Ghiorzi, G.M. Muschik, J. Nat. Products 53 (1990) 1249.
[19] J.H.I. Cardellina, J. Liq. Chromatogr. 14 (1991) 659.
[20] M.G. Nair, US Patent no. 5 279 949, Jan. 18, 1994.

[21] K.V. Ran, US Patent no. 5 380 916, Jan. 10, 1995.
[22] D.-J. Wu, Ph.D. Thesis, Purdue University, West Lafayette, IN, May 1999.
[23] D.-J. Wu, Y. Xie, Z. Ma, N.-H.L. Wang, Ind. Eng. Chem. Res. 37 (1998) 4023.
[24] S.F. Chung, C.Y. Wen, AIChE J. 14 (1968) 857.
[25] E.J. Wilson, C.J. Geankoplis, Ind. Eng. Chem. Fundam. 5 (1966) 9.
[26] Z. Ma, D. Tanzil, B.W. Au, N.-H.L. Wang, Biotech. Prog. 12 (1996) 810.
[27] V. Bringi, P.G. Kadkade, C.L. Prince, B.F. Schubmehl, E.J. Kane, B. Roach, US Patent no. 5 407 816, April 18, 1995.
[28] T. Mallmann, B.D. Burns, Z. Ma, N.-H.L. Wang, AIChE J. 44 (1998) 2628.